<Original Paper>

Journal of the Korean Society for Nondestructive Testing, Vol. 33, No. 3: 257-263, 2013
ISSN 1225-7842 / eISSN 2287-402X http://dx.doi.org/10.7779/JKSNT.2013.33.3.257

Initial Second Harmonic Generation in Narrowband Surface Waves by Multi-Line Laser Beams for Two Kinds of Spatial Energy Profile Models: Gaussian and Square-Like

Sungho Choi* and Kyung-Young Jhang**†

Abstract Acoustic nonlinearity of surface waves is an effective method to evaluate the micro damage on the surface of materials. In this method, the A_1 (magnitude of the fundamental wave) and A_2 (magnitude of the second-order harmonic wave) are measured for evaluation of acoustic nonlinearity. However, if there is another source of second-order harmonic wave other than the material itself, the linear relationship between A_1^2 and A_2 will not be guaranteed. Therefore, the second-order harmonic generation by another source should be fully suppressed. In this paper, we investigated the initial second-order harmonic generation in narrowband surface waves by multi-line laser beams. The spatial profile of laser beam was considered in the cases of Gaussian and square-like. The temporal profile was assumed to be Gaussian. In case of Gaussian spatial profile, the generation of the initial second-order harmonic wave was inevitable. However, when the spatial profile was square-like, the generation of the initial second-order harmonic wave was able to be fully suppressed at specific duty ratio. These results mean that the multi-line laser beams of square-like profile with a proper duty ratio are useful to evaluate the acoustic nonlinearity of the generated surface waves.

Keywords: Laser, Surface Waves, Acoustic Nonlinearity, Initial Second-Order Harmonic

1. Introduction

The acoustic nonlinearity of surface waves has been widely studied by many investigators to evaluate microstructural features such as dislocations in physical deformation and precipitates in phase transformation [1-4]. However, most of the reports employed the conventional ultrasonic technique, which involves the use of contact-type transducers that must be in contact with the surface of the material. Such a technique requires not only flat or simply curved material surface, but also couplants. These requirements can be principal causes of experimental errors. To overcome this problem, laser-ultrasonic techniques have been studied for the generation of surface waves [5].

Laser-ultrasonic technique provides a flexible and simple method for non-contact and remote generation of ultrasonic surface waves [6-13]. In our previous paper, we have studied the frequency characteristics of surface wave by single-line pulsed laser beam in one-dimensional for two kinds of spatial energy profile models; Gaussian and square-like [13], where it was shown that the frequency spectrum was single broadband at Gaussian laser beam but main lobe with multiple side lobes at square-like laser beam.

When the acoustic nonlinearity is used to evaluate the microstructural features, narrow bandwidth with tone-burst waves are preferred than broad bandwidth wave. Narrowband tone-burst waves can be easily produced by using array sources [6-12]. In this way, main frequency and harmonic frequencies are determined by selection of array intervals. In

[Received: May 28, 2013, Revised: June 20, 2013, Accepted: June 21, 2013] *Graduate School of Mechanical Engineering, Hanyang University, Seoul 133-791, Korea, **School of Mechanical Engineering, Hanyang University, Seoul 133-791, Korea, †Corresponding Author: kyjhang@hanyang.ac.kr

order to apply the acoustic nonlinear technique, the initial second-order harmonic generation other than the material itself should be fully suppressed to guarantee the linear relationship between A_1^2 and A_2. Our previous paper showed the possibility that the initial second harmonic generation can be suppressed by null point between side lobes of the frequency spectrum by a single laser beam at square-like beam profile with specific duty ratio. However, the previous one-dimensional analysis did not take into account the thermal conduction effect and the temporal profile of the laser beam was assumed to be a delta function. In practical situations, it is necessary to take into account the thermal expansions in three-dimension with the thermal conductions. Also the Gaussian temporal profile of the laser beam should be considered.

In this paper, we investigated the initial second harmonic generation in narrowband surface waves by multi-line laser beams. The spatial profile of laser beam was considered the cases of Gaussian and square-like. The temporal profile was assumed to be Gaussian. The laser-generated surface waves were simulated using a two-dimensional numerical analysis based on the heat transfer and thermo-elastic model. In the numerical model, temperature-dependent properties, such as density, heat capacity, thermal conductivity, thermal expansion coefficient, Young's modulus and Poisson's ratio, were taken into account. Simulation results were obtained in terms of the normalized magnitude of initial second-order harmonic wave at each laser profile and duty ratio. Finally, the influences of laser profile and duty ratio on evaluation of acoustic nonlinearity were discussed.

2. Generation of Narrowband Laser-Generated Surface Waves

The mechanism of laser-generated surface waves is demonstrated by the thermo-elastic

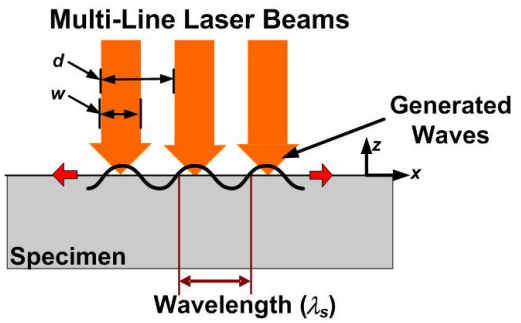

Fig. 1 Schematic diagram of surface waves penetration by multi-line laser beams

effect between a laser beam and a material. When a pulsed laser beam impinges upon a material surface and is partially absorbed into a very thin layer of the surface, extremely fast heating and cooling occur, which leads to the rapid generation of a localized temperature variation. The variation in the rapid thermal expansion of a localized region leads to thermal stress on the surface and the generation of surface elastic waves [5]. Multi-line laser beams can be used to produce tone-burst signal of surface waves. Such a method is advantageous in that the frequency characteristics of the ultrasonic waves may be analyzed. A schematic diagram of surface waves generation by multi-line laser beams is shown in Fig. 1. In the figure, w is the line beam width, d is the line beam separation, and λ_s is the wavelength of the generated surface waves.

The frequency spectrum of the generated surface waves by multi-line laser beams, $G(f)$, can be expressed as follows [14]:

$$G(f) = NH(f)S(f) \tag{1}$$

where N is the number of lined laser beams, $H(f)$ is the frequency spectrum of the surface waves by a single laser beam, and $S(f)$ is the array function.

In general, $H(f)$ depends on laser parameters and material properties. $S(f)$ is the array function which depends on number of lined laser beams N and beam separation d as follows:

$$S(f)=\frac{\sin(\pi Nf\Delta t)}{N\sin(\pi f\Delta t)} \tag{2}$$

where Δt is the time interval between two adjacent slits ($\Delta t=d/c_R$) and c_R is the surface wave speed. From Eq. (2), we can confirm that $S(f)$ spectrum does not depend on the laser profile and laser beam width. It is just dependent on the beam separation d and surface wave speed c_R. These parameters determine the fundamental and second-order frequency by $f_{fund} = c_R/d$ and $f_{second} = 2f_{fund}$. Therefore, in this paper, $S(f)$ was calculated using Eq. (2) and $H(f)$ at each laser profile and duty ratio was simulated using numerical analysis. After that, $G(f)$ was obtained from Eq. (1).

3. Numerical Analysis of Spectrum *H(f)*

The transient temperature distribution $T(x,z,t)$ in the specimens subjected to the laser beam was modeled by classical heat transfer analysis. The 2D differential equation of heat conduction can be represented as follows [5]:

$$\rho C_p\frac{\partial T}{\partial t}-\nabla(k\nabla T)=q \tag{3}$$

where, ρ is the density, C_p is the heat capacity, k is the thermal conductivity, and q is the heat flux as a function of position and time.

The solution of Eq. (3) depends on the heat flux q and the boundary conditions. Here, we assume that the spatial profiles of the laser beam are Gaussian are square-like, and the temporal profile is Gaussian, respectively. That is, the heat flux q can be expressed as follows [5]:

$$\begin{aligned} q_{Gaussian}&=I_0(1-R)\exp\left(-2\frac{x^2}{\left(w/2\right)^2}\right)\exp\left(-2.7726\frac{(t-\tau)^2}{\tau^2}\right) && |x|\le\frac{w}{2}\\ &=0 && |x|>\frac{w}{2}\end{aligned} \tag{4}$$

$$\begin{aligned} q_{Square}&=I_0(1-R)\exp\left(-2.7726\frac{(t-\tau)^2}{\tau^2}\right) && |x|\le\frac{w}{2}\\ &=0 && |x|>\frac{w}{2}\end{aligned} \tag{5}$$

where I_0 is the intensity of the incident beam, R is the reflectivity, and τ is the laser pulse duration.

The equation governing displacement of isotropic media for linear elasticity can be represented as follows [15]:

$$\mu\nabla^2\mathrm{u}+(\lambda+\mu)\nabla(\nabla\cdot\mathrm{u})=\rho\ddot{\mathrm{u}}+(3\lambda+2\mu)\alpha\nabla T \tag{6}$$

where u is the displacement vector field, λ and μ are Lamè constants, ρ is the density, and α is the thermal expansion coefficient. By combining Eqs. (3) and (6), we can calculate the out-of-plane displacement of a laser-generated surface wave.

The frequency response of the generated surface wave was simulated with a 2D symmetric model using COMSOL Multiphysics. Fig. 2 shows the simulation model. The specimen material is aluminum 6061-T6. Boundary 1 is symmetric and the heat flux with a width of $w/2$ is given to the boundary 2. Convection and radiation effects are ignored since the pulse duration is very short; therefore, all boundaries except boundary 1 and 2 are assumed to be insulated. As for mechanical condition, all boundaries are free except boundary 1. The Nd:YAG pulsed laser used in this model has a Gaussian temporal profile. The laser irradiance was fixed at 12.74 mJ/cm^2. The reflectivity of aluminum 6061-T6 at a wavelength of 1064 nm is 0.93 [5].

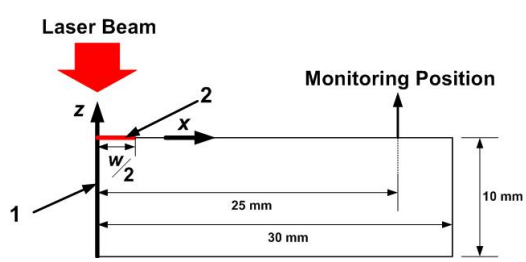

Fig. 2 The 2-D numerical analysis model

Temperature-dependent properties, such as density, heat capacity, thermal conductivity, thermal expansion coefficient, Young's modulus and Poisson's ratio, were taken into account in the numerical model [16,17]. The out-of-plane displacement of surface wave was obtained at a distance 25 mm from the center of the laser beam. A time-dependent solver was used. The time step and mesh size of the FEM analysis limit the frequency range of reliable calculation [18]. The calculation duration was 10 μs in 1 ns intervals and the mesh size was 50 μm. With these parameters, the maximum frequency of reliable calculation is 5 MHz. The initial temperature was 20°C.

4. Simulation Results and Discussion

Fig. 3(a) shows the calculated out-of-plane displacement of the surface wave at Gaussian spatial profile for three typical beam widths: 0.5 mm, 1.0 mm, and 1.5 mm. The frequency response spectra of the time domain signals are shown in Fig. 3(b), which were obtained from

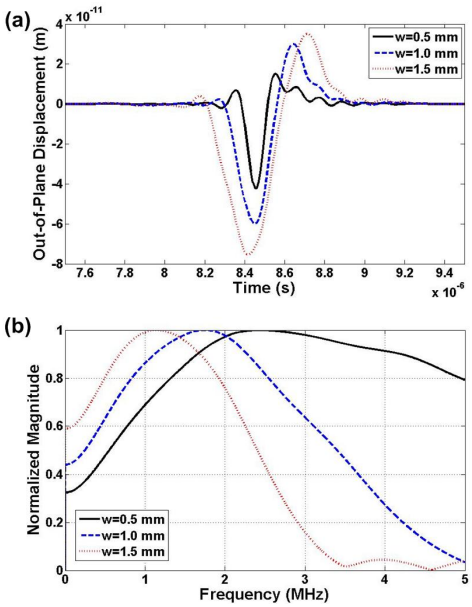

Fig. 3 Three examples of (a) out-of-plane displacement of surface wave and (b) the frequency response spectra at Gaussian spatial profile for w=0.5 mm, 1.0 mm and 1.5 mm

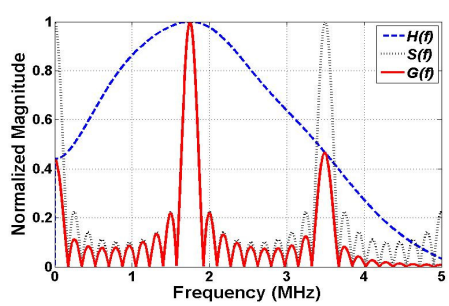

Fig. 4 Typical spectrums of $H(f)$, $S(f)$ and $G(f)$ at Gaussian spatial profile for w=1.0 mm, N=10, d=1.67 mm, and c_R=2920 m/s

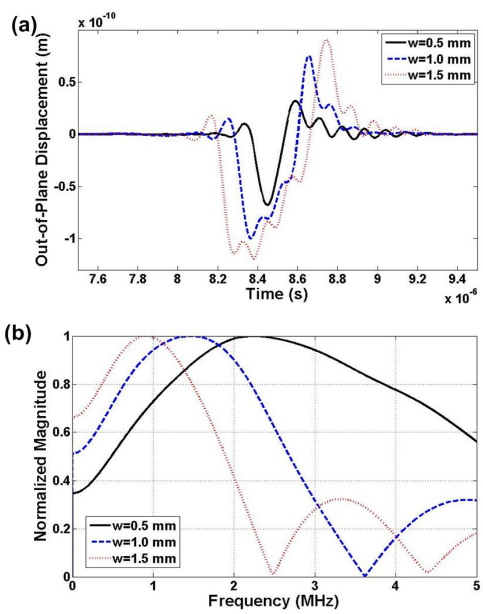

Fig. 5 Three examples of (a) out-of-plane displacement of surface wave and (b) the frequency response spectra at square-like spatial profile for w=0.5 mm, 1.0 mm and 1.5 mm

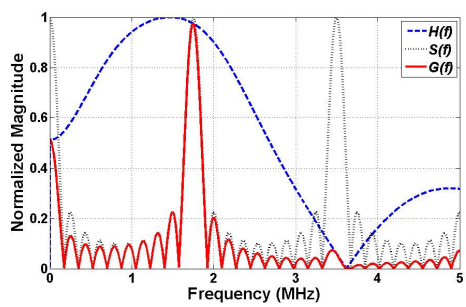

Fig. 6 Typical spectrums of $H(f)$, $S(f)$ and $G(f)$ at square-like spatial profile for w=1.0 mm, N=10, d=1.67 mm, and c_R=2920 m/s

Discrete Fourier Transform at the conditions of 100 MHz sampling rate, zero-padding in 200 times of signal length and hanning window. In these spectra, we can see that the peak frequency moves lower and the bandwidth is more narrow as the beam width increases. This trend is similar with the previous one-dimensional results [13]. However, the band of spectrum is more broad because of considering the thermal conduction effect and the temporal profile of the laser beam.

Typical spectrums of $H(f)$, $S(f)$ and $G(f)$ at $w = 1.0$ mm, $N = 10$, $d = 1.67$ mm, and $c_R = 2920$ m/s are shown in Fig. 4. Both the 1.75 MHz fundamental wave and the 3.5 MHz second-order harmonic wave clearly appear, which means that the second-order harmonic wave is generated initially with the fundamental wave by array function $S(f)$.

Fig. 5(a) shows the calculated out-of-plane displacement of the surface wave at square-like spatial profile for three typical beam widths: 0.5 mm, 1.0 mm, and 1.5 mm. The frequency response spectra of the time domain signals are shown in Fig. 5(b). In these spectra, we can see that multiple peaks appear, and the peak frequencies move lower as the beam width increases. This trend is also similar with the previous one-dimensional results [13]. However, the band of spectrum is more broad and the magnitude of the second peak is lower than that of the first peak. This is also because of considering the thermal conduction effect and the temporal profile of the laser beam. In addition, we can expect that the second harmonic wave can be generated initially similar with the case of Gaussian with the magnitude varying according to the beam width. However, if the zero point between main lobe and side lobe is matched with the second harmonic frequency, the initial second harmonic wave can be suppressed.

Fig. 6 shows typical spectrums obtained at

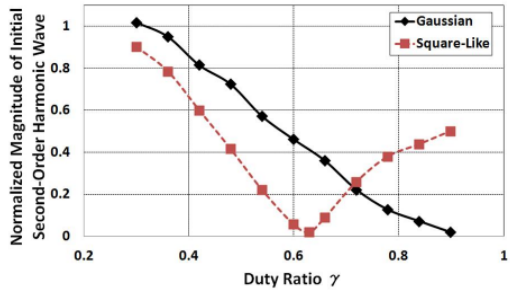

Fig. 7 Variation in normalized magnitude of initial second-order harmonic wave in both the Gaussian and square-like spatial profiles as a function of the duty ratio

$w = 1.0$ mm that is close to such special condition, where other parameters are same with those used in simulation for Gaussian profile. The magnitude of 3.5 MHz second-order harmonic wave clearly decreases compared with the case of Gaussian spatial profile as shown in Fig. 4. This result means that the second-order harmonic wave cannot be generated initially at a specific duty ratio.

The variation in normalized magnitude of initial second-order harmonic wave in both the Gaussian and square-like spatial profile as a function of the duty ratio is shown in Fig. 7. In the case of Gaussian spatial profile, the magnitude of initial second-order harmonic wave monotonically decreases as the duty ratio increases. In the case of square-like spatial profile, however it has a minimum at a specific duty ratio. This means that the generation of the initial second-order harmonic wave can be fully suppressed at this duty ratio. This constraint of initial second-order harmonic wave offers possibility to use measurement of the acoustic nonlinearity in narrowband surface waves generated by multi-line laser beams.

Note that, the duty ratio that minimized A_2 in our study was obtained numerically at the conditions of linear elasticity, perfectly square spatial profile and almost zero of surface roughness. Experimentally, this duty ratio may vary with experimental conditions such as

nonlinear elasticity, sigmoid-like spatial profile and surface conditions. However, we can use the theoretically predicted null point as starting point. It may need try and error to find out actual null point in the experiment.

5. Conclusions

We investigated the initial second harmonic generation in narrowband surface waves generated by multi-line laser beams. The frequency spectrum of surface wave by a single laser beam, $H(f)$ was simulated with a 2D symmetric model in cases that the spatial profile of laser beam was Gaussian and square-like. After that, the frequency spectrum of the generated surface waves $G(f)$ was obtained from a product of $H(f)$ and array function $S(f)$.

Simulation results show that the initial generation of the second-order harmonic wave is inevitable in case of Gaussian spatial profile. On the other hand, in case of square-like spatial profile, the generation of the initial second-order harmonic wave can be fully suppressed at a specific duty ratio. These results mean that the multiple laser beams of square-like profile with a proper duty ratio are useful to evaluate the acoustic nonlinearity of the generated surface waves.

Acknowledgment

This work was supported by the Innovations in Nuclear Power Technology of the Korea Institute of Energy Technology Evaluation and Planning(KETEP) grant funded by the Korea government Ministry of Knowledge Economy. (No. 20101620100080)

References

[1] K. Y. Jhang, J. I. Lee and T. H. Lee, "Acoustic nonlinearity of surface wave in a fatigue aluminum alloy specimen," *Materials Transactions*, Vol. 53, No. 2, pp. 303-307 (2012)

[2] S. V. Walker, K. Y. Kim, J. Qu and L. J. Jacobs, "Fatigue damage evaluation in A36 steel using nonlinear Rayleigh surface waves," *NDT&E International*, Vol. 48, pp. 10-15 (2012)

[3] M. Liu, J. Y. Kim, L. Jacobs and J. Qu, "Experimental study of nonlinear Rayleigh wave propagation in shot-peened aluminum plates - Feasibility of measuring residual stress," *NDT&E International*, Vol. 44, pp. 67-74 (2011)

[4] T. H. Nam, S. H. Choi, T. H. Lee, K. Y. Jhang and C. S. Kim, "Acoustic nonlinearity of narrowband laser-generated surface waves in the bending fatigue of Al6061 alloy," *Journal of the Korean Physics Society*, Vol. 57, No. 5, pp. 1212-1217 (2010)

[5] C. B. Scruby and L. E. Drain, "Laser Ultrasonics: Techniques and Applications," Bristol: Adam Hilger (1990)

[6] A. D. W. McKie, J. W. Wagner, J. B. Spicer and C. M. Penny, "Laser generation of narrow-band and directed ultrasound," *Ultrasonics*, Vol. 27, pp. 323-330 (1989)

[7] J. Huang, S. Krishnaswamy and J. D. Achenbach, "Laser generation of narrow-band surface waves," *Journal of the Acoustical Society of America*, Vol. 92, No. 5, pp. 2527-2531 (1992)

[8] T. W. Murray, J. B. Deaton Jr. and J. W. Wagner, "Experimental evaluation of enhanced generation of ultrasonic waves using an array of laser sources," *Ultrasonics*, Vol. 34, pp. 69-77 (1996)

[9] H. Nishino, Y. Tsukahara, Y. Nagata, T. Koda and K. Yamanaka, "Excitation of high frequency surface acoustic waves by phase velocity scanning of a laser interference fringe," *Applied Physics Letters*,

Vol. 62, No. 17, pp. 2036-2038 (1993)

[10] H. Nakano and S. Nagai, "Laser generation of antisymmetric lamb waves in thin plates," *Ultrasonics*, Vol. 29, No. 3, pp. 230-234 (1991)

[11] D. Royer and E. Dieulesaint, "Analysis of thermal generation of Rayleigh waves," *Journal of Applied Physics*, Vol. 56, No. 9, pp. 2507-2511 (1984)

[12] E. A. Ash, E. Dieulesaint and H. Rakouth, "Generation of surface acoustic waves by means of a C. W. laser," *Electronics Letters*, Vol. 16, No. 12, pp. 470-472 (1980)

[13] H. G. Seo, M. H. Kim, S. H. Choi, C. S. Kim and K. Y. Jhang, "Frequency characteristics of surface wave generated by single-line pulsed laser beam with two kinds of spatial energy profile models: Gaussian and square-like," *Journal of the Korean Society for Nondestructive Testing*, Vol. 32, No. 4, pp. 347-354 (2012)

[14] Y. H. Berthelot and J. Jarzynski, "Directional laser generation and detection of ultrasound with arrays of optical fibers," *Journal of Nondestructive Evaluation*, Vol. 9, No. 4, pp. 271-277 (1990)

[15] I. Arias and J. D. Achenbach, "Thermoelastic generation of ultrasound by line-focused laser irradiation," *International Journal of Solids and Structures*, Vol. 40, No. 25, pp. 6917-6935 (2003)

[16] J. Zimmerman, W. Wlosinski and Z. R. Lindemann, "Thermo-mechanical and diffusion modeling in the process of ceramic-metal friction welding," *Journal of Materials Processing Technology*, Vol. 209, pp. 1644-1653 (2009)

[17] Y. Chao and X. Qi, "Thermal and thermo-mechanical modelling of friction stir welding of aluminium alloy 6061-T6," *Journal of Materials Processing Technology*, Vol. 7, No. 10, pp. 215-233 (1998)

[18] H. Sun, S. Zhang and B Xu, "Influence of viscoelastic property on laser-generated surface acoustic waves in coating-substrate systems," *Journal of Applied Physics*, Vol. 109, pp. 073107 (2011)